Available online at www.sciencedirect.com
ScienceDirect
International Journal of Heat and Mass Transfer 49 (2006) 5018–5026
International Journal of HEAT and MASS TRANSFER
www.elsevier.com/locate/ijhmt

Experimental study of dropwise condensation on plasma-ion implanted stainless steel tubes

A. Bani Kananeh, M.H. Rausch, A.P. Fröba, A. Leipertz *

Lehrstuhl für Technische Thermodynamik (LTT), Universität Erlangen-Nürnberg, Am Weichselgarten 8, D-91058 Erlangen, Germany

Received 26 July 2005; received in revised form 7 March 2006
Available online 7 September 2006

Abstract

Plasma-ion implantation was used to achieve stable dropwise condensation of saturated steam on stainless steel tubes. For the investigation of the efficiency of plasma-ion implantation regarding the condensation process a condenser was constructed in order to measure the heat flux density $\dot{q}$ and the heat transfer coefficient h_c for the condensation of steam on the outside surface of a single horizontal tube. For tubes implanted with a nitrogen ion dose of 10^{16} cm^{-2}, the heat transfer coefficient h_c was found to be larger, by a factor of 3.2, in comparison to values theoretically calculated by the corrected Nusselt film theory. The heat flux density $\dot{q}$ and the heat transfer coefficient h_c were found to increase with increasing ion dose and steam pressure. The heat transfer coefficient decreases with increasing surface subcooling as it has been found in former work for dropwise condensation on ion implanted vertical plates.

Keywords: Dropwise condensation; Heat transfer coefficient; Plasma-ion implantation; Stainless steel tubes; Surface free energy

1. Introduction

Dropwise condensation provides larger heat transfer coefficients compared to filmwise condensation, as discovered in the year 1930 by Schmid et al. [1]. Dropwise condensation can be described as a phenomenon of the incomplete wettability of a surface. The wettability of the surface is responsible for the formation of the respective type of condensation and has a very strong effect on the performance of the heat transfer process. Likewise, the wettability of the surface has a very strong effect on the subcooling of the condensate, for constant cooling performance.

In general, the wettability of a solid surface depends on the interfacial tensions which occur at the phase boundaries between solid–liquid, solid–gas, and liquid–gas. The interfacial tension is a measure for the energy required to form a unit area of new interface. From the free surface energy of a solid which is equivalent to the interfacial tension for the phase boundary solid–vacuum it can be estimated whether a liquid wets a surface or not. When the free surface energy of a solid is low, from 30 to 40 mN m^{-1}, it is relatively unwettable by water which will bead on its surface. If the free surface energy is above 60 mN m^{-1}, the surface will be very wettable and a water drop will spread over a large area with a contact angle below 10° [2].

Although the conditions necessary for promoting dropwise condensation are well known since several decades and experiments with coatings as promoters have been carried out successfully, at least in part, the application of dropwise condensation is still today in a testing phase. The main problems in the realization of dropwise condensation are the insufficiency of the theoretical description of working boundary surface phenomena such as complete or incomplete wettability and their strong dependence on influences caused in the practical operation by contamination, oxidation of the surface, adsorption layers, and gas enclosures.

Dropwise condensation was successfully achieved by Zhao et al. [3,4] using ion implantation of N, Ar, He, H,

* Corresponding author. Tel.: +49 9131 85 29789; fax: +49 9131 85 29901.
E-mail address: sek@ltt.uni-erlangen.de (A. Leipertz).

0017-9310/$ - see front matter © 2006 Elsevier Ltd. All rights reserved.
doi:10.1016/j.ijheatmasstransfer.2006.04.039

Nomenclature

A	area (m^2)
a	constant (m)
c_p	specific heat capacity ($J\ kg^{-1}\ K^{-1}$)
D	diameter (m)
E	modulus of elasticity (Pa)
g	acceleration of gravity ($m\ s^{-2}$)
H_0	overall heat transfer coefficient ($W\ m^{-2}\ K^{-1}$)
h	heat transfer coefficient ($W\ m^{-2}\ K^{-1}$)
K	dimensionless variable in Petukhov–Popow equation (7) (–)
k	thermal conductivity ($W\ m^{-1}\ K^{-1}$)
L	length (m)
Pr	Prandtl number (–)
P	pressure (Pa)
$\dot{Q}$	heat flux (W)
$\dot{q}$	heat flux density ($W\ m^{-2}$)
Re	Reynolds number (–)
S_{surf}	surface entropy ($N\ m^{-1}\ K^{-1}$)
U_{surf}	internal energy of the surface ($N\ m^{-1}$)
T	temperature (K)

Greek symbols

γ	surface energy ($N\ m^{-1}$)
ρ	density ($kg\ m^{-3}$)
ξ	dimensionless variable in Petukhov–Popow equation (7) (–)
μ	dynamic viscosity (Pa s)
Δ	difference (–)
Δh	evaporation enthalpy ($J\ kg^{-1}$)

Subscripts

c	condensation
cw	cooling water
DWC	dropwise condensation
FWC	filmwise condensation
i	inside
in	inlet conditions
LMTD	logarithmic mean temperature difference
o	outside
out	outlet conditions
p	constant pressure
s	steam
sat	saturation
sub	subcooling
surf	surface
w	wall of the tube

Abbreviations

DWC	dropwise condensation
FWC	filmwise condensation
LMTD	logarithmic mean temperature difference
PTFE	polytetrafluoroethylene

and Cr in copper tubes. Zhao and Burnside [5] implanted PTFE coated tube surfaces with Cr^+ and obtained heat transfer coefficients five times larger than those of unimplanted tubes. The method of simultaneous magnetron sputtering ion-plating of Cr^+ and N^+ and then of CH_4 in copper U-tubes [6] and C_2H_6 in white copper (70%Cu:30%Ni) U-tubes [7] produced excellent DWC of steam.

Also at our institute successful work has been carried out to achieve dropwise condensation on metallic surfaces by using the method of ion-beam implantation. Stable dropwise condensation can be achieved on metallic surfaces by an appropriately implemented ion-beam implantation process with an ion dose of $10^{15}\ cm^{-2}$, using nitrogen ions. Investigations on ion-implanted condenser plates have shown condensate heat transfer coefficients up to 17 times larger than those obtained by filmwise condensation [8].

The major goal of this work is the usage of plasma-ion implantation for achieving stable dropwise condensation on horizontal condenser tubes, which may allow the future technical application of DWC. The increase in the condensation heat transfer coefficients of steam over these tubes is determined experimentally.

2. Reduction of the surface energy of metals by ion implantation

Due to their strong bondings, metal surfaces usually possess a high surface free energy ($\gamma_{surf} \sim 0.5$–$5\ N\ m^{-1}$) which is given by

$$\gamma_{surf} = U_{surf} - TS_{surf}. \quad (1)$$

The surface free energy γ_{surf} can be decreased both by decreasing the surface's total energy U_{surf} and by increasing the surface entropy S_{surf}. The implantation of foreign elements into the surface can increase S_{surf}. If the implanted elements have a sufficiently high kinetic energy, the interatomic bond energy of the surface layer will be decreased and hence, U_{surf} will be reduced. The higher the kinetic energy of the elements implanted, the more is the decrease in the surface free energy of the implanted surface [5]. The surface free energy depends on the chemical valence and the ionic radius of the positive ions implanted. The smaller the radius and the higher the valence, the lower the surface free energy becomes [9].

Implanting certain elements into a metal surface may cause transition of the metal surface layer from the crystalline to the amorphous state. The latter state is more

disordered and has weaker inter-atomic forces than the crystalline state. The modulus of elasticity E of the amorphous state metal is about 20–30% smaller than that one of the crystalline state [5], consequently the surface free energy γ_{surf} of the amorphous state metal is lower than that one of the crystalline state metal, which can be seen by

$$\gamma_{surf} = \frac{Ea_o}{4\pi^2}, \tag{2}$$

where a_o is a constant. Ion-beam implantation technology has been used by Zhao et al. [4] to develop a non-wetting Cu surface by implantation of Cr^+ and N^+. A metallographic examination of the surface layer has shown that the normal crystalline structure of Cu was transferred into an amorphous state with an accompanying reduction of 30% in its elasticity.

3. Experimental

Experiments have been performed to quantitatively describe the heat transfer process for DWC of saturated steam on ion-implanted horizontal tubes. An experimental condenser has been constructed to measure the condensation heat transfer coefficient on different tubes. Figs. 1 and 2 show a schematic diagram of the experimental apparatus and of the condenser cell, respectively. The experimental apparatus consists mainly of four parts, an evaporator with automatic water supply, a condenser test cell, a cooling water cycle, and a condensate collection and recycling system. The outside diameter of the condenser shell is 324 mm with a wall thickness of 5 mm. The condenser shell diameter is selected so that it is large enough for the visual observation of the whole surface of the tube through the condenser windows. All parts of the apparatus, the condenser test cell, the steam lines, the condensate lines and the cooling water lines, are thermally insulated using fiber glass in order to reduce the heat losses to the surroundings which influence the heat transfer measurements during the condensation process.

The saturated steam is produced by the evaporator (2), which is heated by four electric heating elements (8). The steam pressure inside the evaporator is regulated by a thyristor plate connected to the electric heating elements. The steam pressure inside the condenser is regulated using a manual reducing valve installed on the steam line to the condenser. The steam pressure is measured with a calibrated pressure transducer with an accuracy of 0.1%. All temperatures of the experimental apparatus including the steam temperature are measured using calibrated resistance thermometers Pt100-Ω with an absolute uncertainty of ±0.1 K. The relative uncertainty of the resistance probes among each other was less than ±0.01 K. The water level inside the evaporator is controlled by a level controller connected with the supplying pump (6), which feeds deionized water from the storage tank (7) to the evaporator. The steam condenses at the outside of the condenser tube and the condensate is collected on the collection plate (24), see Fig. 2. The condensate flows out of the condenser to a steam trap (4), where the condensate is separated from the steam and where its temperature is measured. The condensate is cooled by the condensate cooler (13) and its mass flow is measured manually by weighing the condensate collected within a certain time. Then, the condensate is recycled to the storage tank (7) by the condensate pump (15). The condensate formed on the condenser walls is taken out separately from the bottom of the condenser so that it does not affect the measurement of the condensate mass flow resulting at the condenser tube. The cooling water flows through the condenser in a counter flow arrangement with the steam, and the temperatures at the cooling water inlet and outlet are measured. The cooling water is well mixed by using a water mixer installed inside the cooling water lines to guarantee, on the one hand, a homogeneous temperature at the measurement points and, on the other

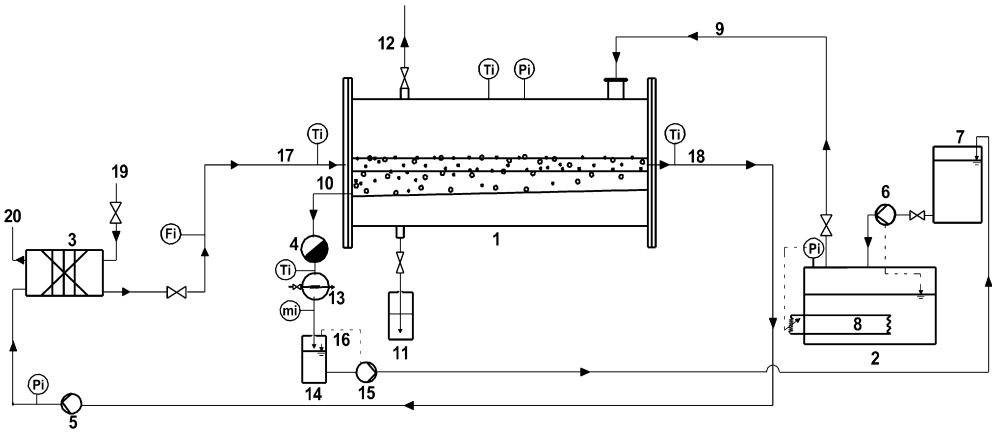

Fig. 1. Schematic diagram of the experimental apparatus: (1) condenser, (2) evaporator, (3) plate heat exchanger, (4) steam trap, (5) cooling water pump, (6) evaporator feed water pump, (7) water tank, (8) electric heater, (9) steam feed to the condenser, (10) condensate from the condenser tube, (11) condensate from the condenser shell, (12) venting, (13) condensate cooler, (14) condensate collection tank, (15) condensate pump, (16) level controller, (17) cooling water into the condenser, (18) cooling water out of the condenser, (19) cooling water into the plate heat exchanger, (20) cooling water out of the plate heat exchanger, (Ti) resistance thermometer Pt100-Ω, (Fi) flow meter, (mi) mass flow measurement.

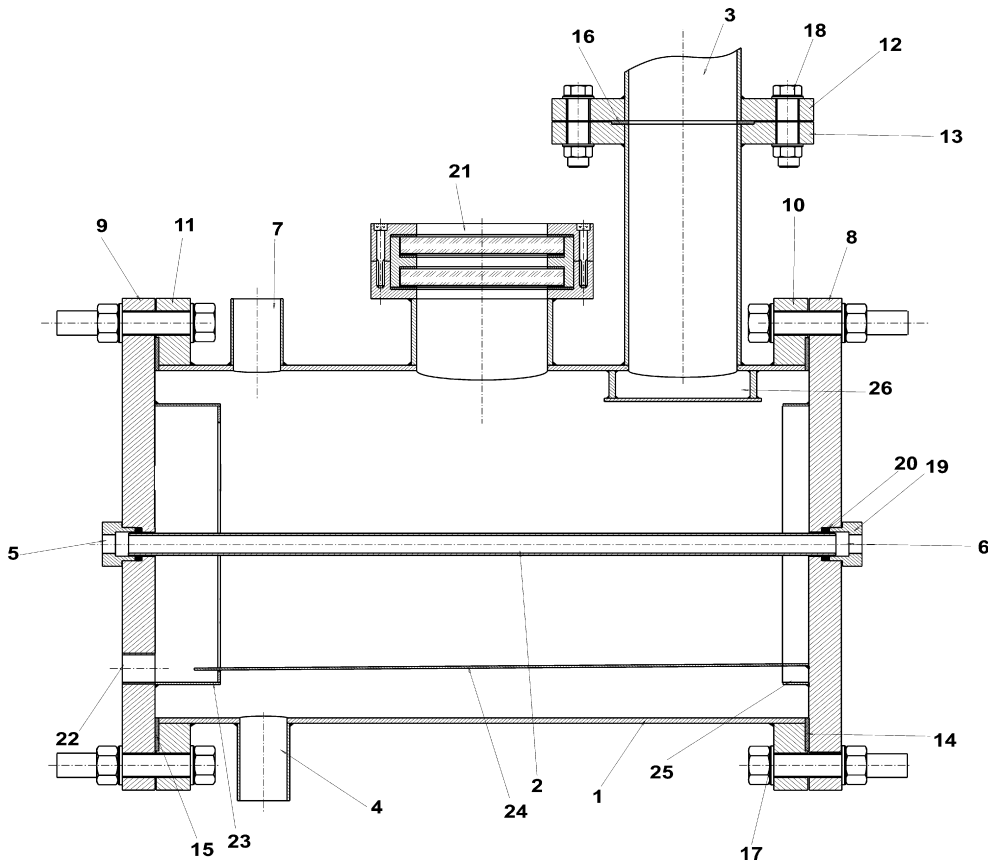

Fig. 2. The condenser cell: (1) condenser shell, (2) condenser tube, (3) steam inlet, (4) condensate outlet from condenser shell, (5) cooling water inlet, (6) cooling water outlet, (7) venting, (8,9) tube sheets, (10,11,12,13) flanges, (14,15,16) PTFE gaskets, (17,18) bolts, (19) tube bushing, (20) rubber O-ring, (21) sight glass, (22) condensate outlet, (23,24,25) condensate collection parts, (26) impingement plate.

hand, to additionally contribute to the fully developed turbulent flow through the condenser tube. The cooling water is pumped to the condenser by a water pump (5) passing a plate heat exchanger, where it is cooled in counter flow with the cooling water coming from an external cooling system. The cooling water flow rate is measured with a magnetic-inductive volume flow meter with an inaccuracy of ±0.5%. From the inaccuracies of the measurement equipment and the long term stabilities of the quantities obtained during the experiments, the maximum uncertainties of the directly measured values are estimated to be $\pm 0.2\,\mathrm{l\,min^{-1}}$ for the cooling water flow rate, $\pm 0.06\,\mathrm{g\,s^{-1}}$ for the condensate mass flow rate, ±5 mbar for the steam pressure, and ±0.2 K for all measured temperatures.

3.1. Tube surface preparation

The used condenser tubes have a length of 500 mm, an outer diameter of 20 mm, and a wall thickness of 2 mm. Because of its high stability against corrosion, stainless steel X 10 Cr Ni Mo 18 9 (material no. 1.4571, thermal conductivity $16.3\,\mathrm{W\,m^{-1}\,K^{-1}}$) was used as substrate material in the experiments. Dropwise condensation was examined by employment of the same tube material treated with plasma-ion implantation, where a plasma is created by a high voltage surrounding the tubes, where subsequently the ion implantation is induced. Nitrogen ions (N) were selected as doping elements with ion doses of 10^{15} and $10^{16}\,\mathrm{cm^{-2}}$. This element was chosen, on the one hand, because of economical reasons, and on the other hand, due to the long time stability of dropwise condensation on N^+ implanted plates, as was found by Leipertz et al. [8].

3.2. Establishment of filmwise condensation (FWC)

Filmwise condensation was established on unimplanted tubes to prove the cleanliness of the apparatus. A condensing film covering the whole surface of the unimplanted tubes indicates that no impurities are present on their surface. If impurities are present, formation of condensate drops will occur. In this way it can be guaranteed that dropwise condensation on the implanted tubes is caused only by the modification of the tubes' surface.

In order to remove contaminations from the condenser walls and from the steam pipe between evaporator and condenser, the complete apparatus was cleaned with 5% NaOH lye at 60 °C, for a period of several hours. After discharging the NaOH lye, the apparatus was washed with tap water several times and then rinsed with distilled water for several hours. The unimplanted tube was well cleaned in an

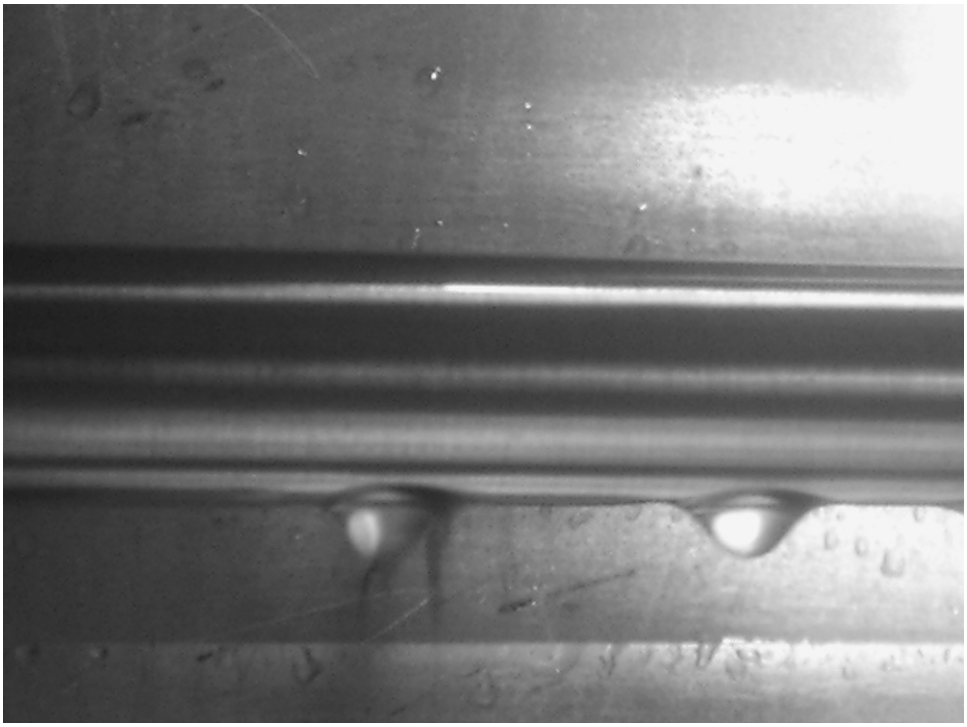

Fig. 3. FWC on an unimplanted stainless steel tube.

ultrasonic bath with a special cleaner to remove any fat, oil, or any other impurities from the tube's surface. Afterwards, the tube was washed with tap water several times, rinsed with acetone, and finally rinsed with distilled water. After the cleaning procedure, the tube was installed and a condensate film covered the surface completely, as shown in Fig. 3. In addition, a chemical analysis of the feed water and of the condensate confirmed the absence of organic contaminations which might promote DWC.

4. Data evaluation – heat transfer coefficient

The overall heat transfer coefficient H_o in a tube-condenser can be determined by

$$H_o = \frac{\dot{Q}}{A \cdot \Delta T_{LMTD}}, \tag{3}$$

where $\dot{Q}$ is the total heat flow, ΔT_{LMTD} the log mean temperature difference, and A the area of the outer tube surface. ΔT_{LMTD} can be calculated by

$$\Delta T_{LMTD} = \frac{T_{cw,out} - T_{cw,in}}{\ln\left(\frac{T_s - T_{cw,in}}{T_s - T_{cw,out}}\right)}, \tag{4}$$

where T_s is the saturated steam temperature and $T_{cw,in}$ and $T_{cw,out}$ are the inlet and outlet cooling water temperatures, respectively. $\dot{Q}$ can be determined from the energy balance on either the condensate side or the cooling water side. The total heat flow on the cooling water side $\dot{Q}_{cw}$ can be determined as

$$\dot{Q}_{cw} = \dot{m}_{cw} c_{p,cw} (T_{cw,out} - T_{cw,in}), \tag{5}$$

where $\dot{m}_{cw}$ is the mass flow rate of the cooling water and $c_{p,cw}$ is its specific heat capacity. The total heat flow on the condensate side $\dot{Q}_c$, including the subcooling, can be determined as

$$\dot{Q}_c = \dot{m}_c [\Delta h + c_{p,c}(T_s - T_c)], \tag{6}$$

where $\dot{m}_c$ is the condensate mass flow rate, $c_{p,c}$ its specific heat, and Δh the evaporation enthalpy. The two values of the total heat flow $\dot{Q}_{cw}$ and $\dot{Q}_c$ should be equal; their difference was smaller than 5% in all experiments. $\dot{Q}_c$ has a higher accuracy than $\dot{Q}_{cw}$, and so, the investigations of the heat transfer calculations in this work will be done relative to the condensate side.

The convective heat transfer coefficient for the cooling water inside the tube h_{cw} was calculated with the Petukhov–Popov correlation [10]

$$h_{cw} = \frac{k_{cw}}{D_i} \frac{(\xi/8) Re\, Pr}{K_1(\xi) + K_2(Pr)(\xi/8)^{1/2}(Pr^{2/3} - 1)}, \tag{7}$$

where $\xi = (0.79 \ln Re - 1.64)^{-2}$, $K_1(\xi) = 1 + 3.4\xi$, and $K_2(Pr) = 11.7 + 1.8 Pr^{-1/3}$. k_{cw} is the thermal conductivity of the cooling water and D_i the inner diameter of the condenser tube. The Petukhov–Popov correlation is valid for fully developed turbulent flow inside a smooth tube. The range of validity includes $Re = 10^4$–10^6 and $Pr = 0.5$–2000. The prediction of h_{cw} by Eq. (7) shows deviations within 1% from the most accurate experimental data, except for the range with Reynolds numbers between 5×10^5 and 5×10^6 and Prandtl numbers between 200

and 2000, where deviations of up to 2% can be found [10]. In this study, turbulent flow for the cooling water was ensured by keeping $Re > 10^4$.

The overall heat transfer coefficient H_o is related to the inner (water) and outer (condensate) heat transfer coefficients, h_{cw} and h_c, by the Péclet-equation

$$\frac{1}{H_o A_o} = \frac{1}{h_{cw} A_i} + \frac{\ln(D_o/D_i)}{2\pi L k_w} + \frac{1}{h_c A_0}, \tag{8}$$

where k_w is the thermal conductivity of the condenser tube wall, D_o the outer diameter of the condenser tube, L its length, and A_i and A_o the inner and outer area of the condenser tube, respectively. The condensation heat transfer coefficient h_c can thus be calculated from Eq. (8) by

$$h_c = \left(\frac{1}{H_0} - \frac{1}{h_{cw}(D_i/D_o)} - \frac{\ln(D_o/D_i)}{2k_w/D_o} \right)^{-1}. \tag{9}$$

The subcooling ΔT_{sub}, which is the temperature difference between the steam and the outer tube surface, is difficult to measure directly without influencing the condensation process. Additionally, the local surface temperature varies with the size of the drops present and also due to the unsteady drop growth and its removal with time. For these reasons, the tube's surface temperature T_{surf} was not measured directly in this work. However, using the definition for the heat transfer coefficient the subcooling ΔT_{sub} and by this the tube's surface temperature T_{surf} can be calculated by

$$\Delta T_{subc} = T_s - T_{surf} = \frac{\dot{Q}_c}{h_c \cdot A_o}. \tag{10}$$

In the next section, our experimental results of the heat transfer coefficient on ion-implanted horizontal tubes will also be discussed in comparison to FWC. The heat transfer coefficient for FWC h_{FWC} for a single horizontal tube can be calculated from Nusselt's film theory [11]

$$h_{FWC} = 0.728 \left[\frac{\Delta h \rho_c (\rho_c - \rho_s) g k_c^3}{\mu_c (T_s - T_{surf}) D_o} \right]^{1/4}, \tag{11}$$

where ρ_c and ρ_s are the densities of condensate and steam, respectively, k_c is the thermal conductivity of the condensate, μ_c its viscosity, and g is the acceleration of gravity.

5. Results and discussion

Experiments were carried out on an unimplanted tube and on tubes implanted with ion doses of 10^{15} and 10^{16} N cm^{-2}. Different conditions were investigated by varying the cooling water flow rate and thus the subcooling at steam pressures of about 1000, 1500, and 2000 mbar. The cooling water volume flow rate was set in steps of 5 l min^{-1} between 10 and 50 l min^{-1}.

5.1. Results for FWC

The first experiments were carried out for an unimplanted tube on which FWC was formed. The results

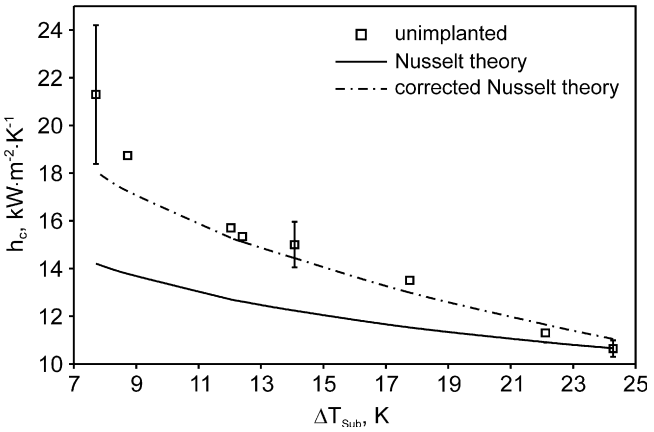

Fig. 4. Experimental values of the heat transfer coefficient h_c on an unimplanted tube at a steam pressure of 1050 mbar as a function of subcooling, in comparison with theoretically calculated values for FWC.

obtained for the heat transfer coefficients at a steam pressure p_s of 1050 mbar are shown in Fig. 4. Here, also the theoretical values for h_c are shown, which have been calculated using Eq. (11). It can be seen that the experimental values of the heat transfer coefficient are larger than those calculated by the Nusselt film theory. In developing Eq. (11), it is assumed that the condensate flow forms a continuous film on the bottom part of the tube. This part of the tube is then associated with an infinite thermal resistance resulting in a decrease in the average heat transfer coefficient [12]. Visual observations inside the condenser cell have shown that at lower subcooling the condensate film does not cover the whole surface of the tube. Some parts of the film were fractured, thus causing an increase in the heat transfer from the steam to the tube surface. At higher subcooling a steady film was observed over the whole surface, resulting in a decrease of the measured heat transfer coefficients, which therefore approached the values calculated theoretically according to Eq. (11), as can be seen in Fig. 4. Here the exemplarily depicted error bars have been calculated by a Gaussian error propagation where the maximum uncertainties of the individual quantities have been taken into account.

The determined errors in the condensate heat transfer coefficient were between 3% and 13% and depend on the subcooling. The maximum value was 13% at ΔT_{sub} of 7.7 K where the maximum condensate heat transfer coefficient was attained. The increase in the relative error at low subcoolings can be explained by the increase in the error in the determination of the surface temperature of the tube T_w, which was calculated by the method explained in Section 4.

The deviation of the experimental values of the heat transfer coefficients from the theoretical values calculated by the Nusselt film theory can be minimized by applying certain corrections to the Nusselt theory. The effect of turbulence, the condensate subcooling, the ripples, the variable properties of the condensate and the inertia forces cause the experimental values to deviate from the Nusselt

theory. The effect of the condensate subcooling was already taken into consideration for the calculation of the experimental heat transfer coefficients. The effect of turbulence could be excluded also because the range of the condensate Reynolds numbers was between 48 and 100. They are below 400 which is the limit value for the condensate turbulence [13]. Actually, three remaining correction factors had to be included in the calculation of the theoretical values of the heat transfer coefficients by Nusselt's theory. The first one is for the ripples formed on the condensate surface which enhances the heat transfer, $h_{\mathrm{FWC,wavy}} = f \cdot h_{\mathrm{FWC}}$. A factor of 1.15 has been taken as an average for the calculation of the heat transfer coefficient [13]. The second factor is related to the variation of the physical properties of the condensate with temperature, especially for the viscosity of the condensate. The third factor is the effect of the inertia forces. The corrected film heat transfer coefficients were calculated by

$$\frac{h_{\mathrm{FWC,corrected}}}{h_{\mathrm{FWC}}} = 1.15\left\{\frac{1+\mu_c^*}{10(1+k_c^*)^3}\left[5+k_c^*(14+11\cdot k_c^*)+\frac{k_c^*}{\mu_c^*}(1+4\cdot k_c^*+5\cdot k_c^{*2})\right]\right\}\cdot\left\{0.0203\left[\frac{\Delta h\cdot\mu_c}{k_c(T_s-T_w)}\right]^{0.5}+0.79\right\}, \quad (12)$$

where $k_c^* = k_{c,sat}/k_{c,w}$ and $\mu_c^* = \mu_{c,sat}/\mu_{c,w}$.

The corrected theoretical values are shown in Fig. 4. It can be seen that the corrected values of the Nusselt theory have approached most of the experimental values. The deviation between the experimental values and the corrected theoretical ones was between 1.5% and 15.1%. The maximum deviation was at low subcooling of 7.7 K where the condensate film was fractured and did not cover the whole surface of the tube, as was explained before.

5.2. Results for DWC

For the establishment of DWC, a stainless steel tube implanted with an ion dose of 10^{16} N cm^{-2} was built into the condenser. The same cleaning procedure applied for the unimplanted tube was applied for the implanted one. Also, the same cleaning procedure for the evaporator and the complete apparatus was applied here.

At small cooling water flow rates of 10 l min^{-1}, stable DWC was achieved on the stainless steel tube implanted with an ion dose of 10^{16} N cm^{-2}, as shown in Fig. 5. At larger cooling water flow rates of 40–50 l min^{-1}, a mixed form of condensation between FWC and DWC was observed. This can be attributed to the increased formation of condensate drops on the surface of the tube. More condensate is removed, whereby the surface of the tube is continuously covered with condensate. The appearance of this form of condensation looks like a stream of condensate between the drops.

5.2.1. Effect of the ion dose

The measured heat transfer coefficients at a steam pressure p_s of 1050 mbar for two implanted tubes with different ion doses are shown in Fig. 6 as a function of the subcooling. The heat transfer coefficient decreases with increasing subcooling because the amount of condensate on the tube's surface increases. The resulting additional heat conduction resistance for the heat transfer from the steam to the surface of the tube is responsible for this effect. For large subcoolings, the heat transfer coefficients for DWC approach the values for FWC. These results are in agreement with the investigations made for hard coated surfaces [14,15], but disagree with those obtained previously for ion-implanted surfaces using ion-beams for the implantation [16].

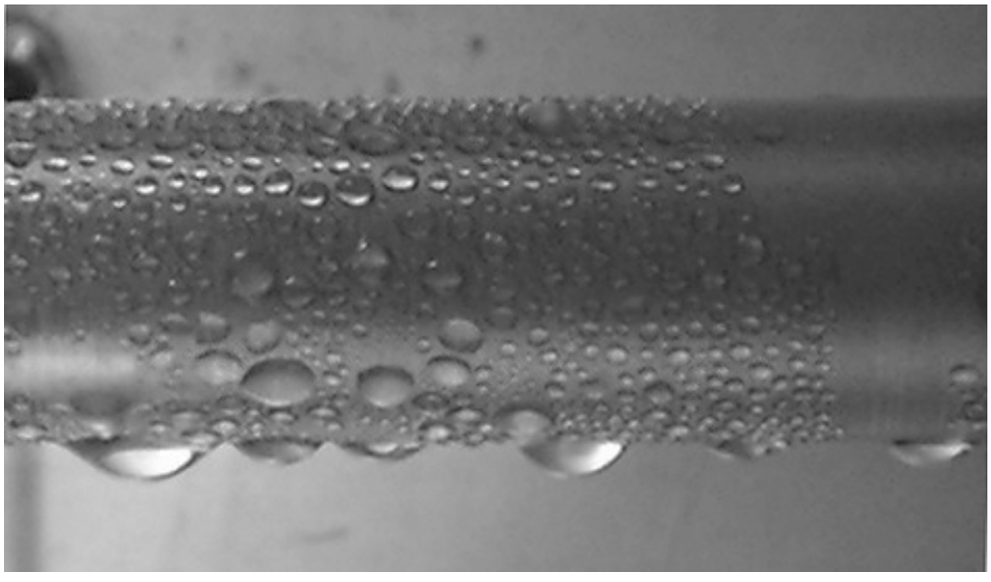

Fig. 5. DWC on an implanted tube with an ion dose of 10^{16} N cm^{-2}.

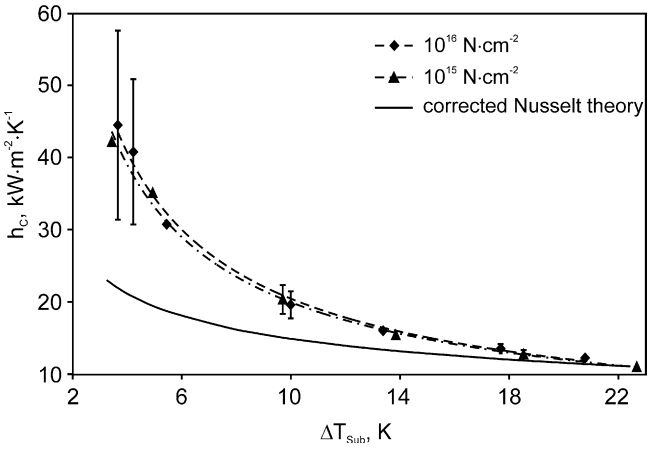

Fig. 6. Measured heat transfer coefficient h_c on implanted tubes with different ion doses at a steam pressure of 1050 mbar as a function of subcooling, in comparison with theoretically calculated values for FWC by corrected Nusselt theory.

Increasing the ion dose increases the heat transfer coefficient. This is due to the decrease in the surface free energy, which reduces the wettability of the surface, as discussed in Section 2. The heat transfer coefficient h_c for DWC was found to be larger by a factor of 3.2 and 2.2, in comparison to FWC calculated from corrected Nusselt's film theory, for ion doses of 10^{16} and 10^{15} N cm^{-2}, respectively.

Fig. 7 shows the measured heat flux density in dependence on the subcooling for the two different ion doses. It can be seen that the heat flux density increases with increasing subcooling. At larger subcoolings, faster drop growth and drop combination were obtained, leading to faster drop removal from the surface. Consequently, the free surface increases on which small drops are again formed which positively affects the heat transfer. On the other hand, faster drop growth as well as an intensified drop combination leads to a more frequent formation of larger drops, whereby an additional heat conduction resistance for the heat transfer from the steam to the tube's surface is produced. Both effects act in opposite directions. The increase in the amount of condensate at the tube's surface can explain the reduction in the heat transfer coefficient, while the increase in the free surface of the tube increases the heat flux density.

The maximum relative error in the determination of the heat flux density was about 1.3% which can be considered as an accurate value. On the other hand, the relative error in the determination of the subcooling, which is determined from the heat flow on the steam side and the condensate heat transfer coefficient h_c, was between 5 and 35% and depends on the value of the subcooling. At small subcooling of about 3.5 K the maximum error was about 35%, while at larger subcooling of 23.0 K the relative error was not more than 5%. The high relative error at low subcoolings can be explained by the increase in the error in the determination of the surface temperature of the tube T_w, which was calculated by the method explained in Section 4. The relative error in T_w depends on many other errors, some of them are the uncertainties in the measurements of the temperatures and of the mass flows, and others on the determination of the cooling water side heat transfer coefficient. The uncertainties in the measurements of the temperatures have larger effects in this case because their values are significant in comparison with the subcooling. In summary, the heat flux density values are quite exact, while the assigned subcoolings are less accurate so that the heat flux densities are shifted either towards larger or smaller subcooling values.

5.2.2. Effect of pressure

Experiments were carried out for different steam pressures for a tube implanted with an ion dose of 10^{16} N cm^{-2}. The results are shown in Figs. 8 and 9. It can be seen that at constant subcooling the heat flux density and the heat transfer coefficient increase with increasing steam pressure. On one hand, this is caused by the decrease of the interfacial resistance to mass transfer at the liquid–vapor interface

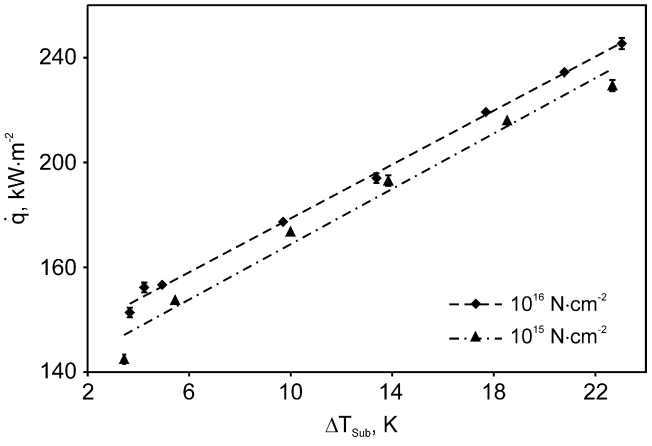

Fig. 7. Measured heat flux density $\dot{q}$ on an unimplanted tube and on implanted tubes with different ion doses at a steam pressure of 1050 mbar as a function of subcooling.

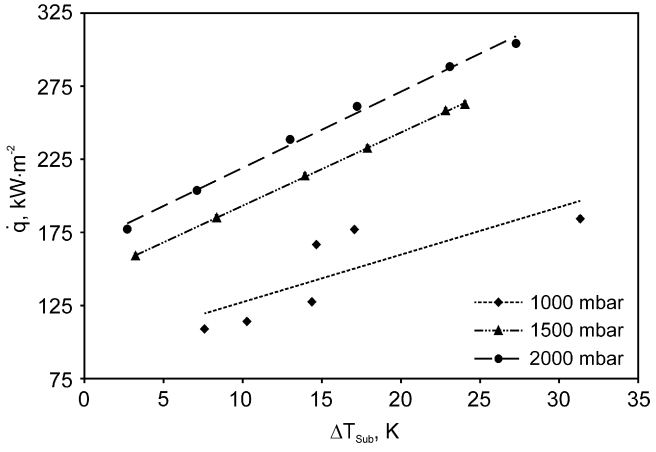

Fig. 8. Measured heat flux density $\dot{q}$ on an implanted tube with an ion dose of 10^{16} N cm^{-2} as a function of subcooling, for different steam pressures.

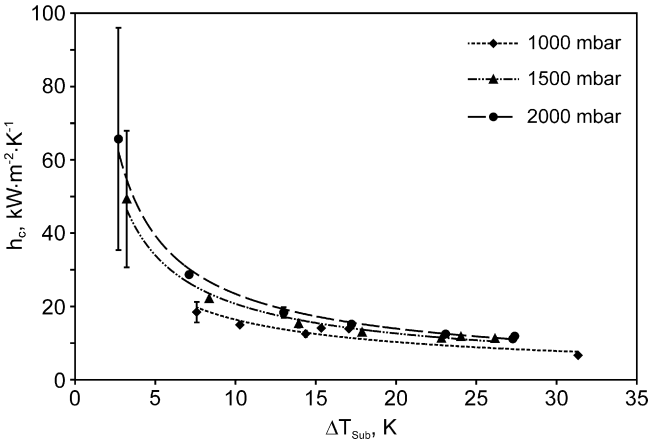

Fig. 9. Measured heat transfer coefficient h_c on an implanted tube with an ion dose of 10^{16} N cm^{-2} as a function of subcooling, for different steam pressures.

with increasing pressure [17]. On the other hand, by increasing the steam pressure, the steam temperature increases leading to a decrease in the surface tension of the condensate [18]. By this, the drop running off diameter is reduced, thus increasing both the heat flux density and the heat transfer coefficient.

6. Conclusions

Stable DWC was obtained on stainless steel tubes implanted with ion doses of 10^{15} and 10^{16} N cm^{-2} at low cooling water flow rates which converted at higher cooling water flow rates to a mixed condensation form of FWC and DWC. The measured heat transfer coefficient h_c for DWC was found to be larger by a factor of about 3 compared with the FWC values calculated from corrected Nusselt's film theory and could be enhanced by increasing the ion dose. An increasing steam pressure has a positive effect on DWC by lowering the interfacial resistance of mass transfer at the liquid–vapor interface as well as the surface tension of the condensate.

References

[1] E. Schmid, Schurig, W. Sellschopp, Versuche über die Kondensation von Wasserdampf in Film- und Tropfenform, Tech. Mech. Thermodyn. 1 (2) (1930) 53–63.

[2] J.R. Roth, Industrial Plasma Engineering: Application to Nonthermal Plasma Processing, vol. 2, IOP Publishing Ltd, London, 2001.

[3] Q. Zhao, D.C. Zhang, J.F. Lin, Surface materials with dropwise condensation made by ion implantation technology, Int. J. Heat Mass Transfer 34 (11) (1991) 2833–2835.

[4] Q. Zhao, D.C. Zhang, X.B. Zhu, D.Q. Xu, Z.Q. Lin, J.F. Lin, Industrial application of dropwise condensation, in: Proc. 9th Int. Heat Transfer Conf., vol. 4, 1990, pp. 391–394.

[5] Q. Zhao, B.M. Burnside, Dropwise condensation of steam on ion implanted condenser surfaces, Heat Recov. Syst. CHP 14 (5) (1994) 525–534.

[6] Q. Zhao, D.C. Zhang, S.D. Li, D.Q. Xu, J.F. Lin, G.Q. Li, G.Q. Wang, Dropwise condensation of steam on ion-plating surface, in: Proc. of Int. Conf. on Petroleum Refining and Petrochemical Processing, vol. 2, 1991, pp. 1049–1052.

[7] Q. Zhao, J.J. Liu, T. Bai, J.F. Lin, B.Y. Cui, J.L. Shen, N.T. Fang, Dropwise condensation of steam on vertical and horizontal U-type tube condensers, in: Proc. 10th Int. Heat Transfer Conf., 1994, pp. 117–121.

[8] A. Leipertz, K.-H. Choi, L. Diezel, Dropwise condensation heat transfer on ion implanted metallic surfaces, in: Proc. 12th Int. Heat Transfer Conf., vol. 3, 2002, pp. 887–892.

[9] D. Zhang, Z. Lin, A new method for achieving dropwise condensation, J. Chem. Ind. Eng. (China) 3 (2) (1988) 263–280.

[10] B.S. Petukhov, Heat transfer and friction in turbulent pipe flow with variable physical properties, Adv. Heat Transfer 6 (1970) 503–564.

[11] J.W. Rose, Film condensation, in: S.G. Kandlikar, M. Shoji, V.K. Dhir (Eds.), Handbook of Phase Change: Boiling and Condensation, Taylor & Francis, Philadelphia, 1999, pp. 523–580 (Chapter 19).

[12] M. Belghazi, A. Bonnetemps, J.C. Signe, C. Marvillet, Condensation heat transfer of a pure fluid and binary mixture outside a bundle of smooth horizontal tubes, Int. J. Refrig. 24 (2001) 841–855.

[13] K. Stephan, Heat Transfer in Condensation and Boiling, Springer-Verlag, New York, 1992.

[14] G. Koch, D.C. Zhang, A. Leipertz, Condensation of steam on the surface of hard coated copper discs, Heat Mass Transfer 32 (1997) 149–156.

[15] G. Koch, D.C. Zhang, A. Leipertz, M. Grischke, A. Trojan, H. Dimigen, Study on plasma enhanced CVD coated material to promote dropwise condensation of steam, Int. J. Heat Mass Transfer 41 (13) (1998) 1899–1906.

[16] A. Leipertz, K.H. Choi, Dropwise condensation on ion implanted metallic surfaces, in: Proc. 3rd European Thermal Sciences Conf., 2000, pp. 917–920.

[17] J.W. Rose, Y. Utaka, I. Tanasawa, Dropwise condensation, in: S.G. Kandlikar, M. Shoji, V.K. Dhir (Eds.), Handbook of Phase Change: Boiling and Condensation, Taylor & Francis, Philadelphia, 1999, pp. 581–591 (Chapter 20).

[18] A.K. Das, H.P. Kilty, P.J. Marto, G.B. Andeen, A. Kumar, The use of an organic self-assembled monolayer coating to promote dropwise condensation of steam on horizontal tubes, J. Heat Transfer 122 (2000) 278–286.